Research Article

Peitu Shengjin Recipe Attenuates Airway Inflammation via the TLR4/NF-kB Signaling Pathway on Chronic Obstructive Pulmonary Disease

Xuzhen Hu (ID)**, Bo Hong** (ID)**, and Minghuan Sun** (ID)

Respiratory Department, Ningbo City Hospital of Traditional Chinese Medicine, Ningbo, Zhejiang 315000, China

Correspondence should be addressed to Xuzhen Hu; huxuoo@163.com

Background. Chronic obstructive pulmonary disease (COPD) is a common respiratory disease, but there is no specific medicine for COPD. In this study, we aimed to evaluate the effects of Peitu Shengjin Recipe (PSR) and Biostime Probiotic Powder on COPD rats. *Methods.* UPLC-Q/TOF-MS was used to detect the chemical constituents in PSR. The COPD rat model was established by cigarette smoke combined with tracheal injection of lipopolysaccharide. We assessed lung function by calculating $FEV_{0.3}$/FVC%, dynamic lung compliance (Cdyn), and resistance of inspiration (RI). Histological analysis was performed by HE staining. The levels of TNF-α, IFN-γ, IL-1β, IL-4, and IL-10 were detected by the ELISA. The mRNA and protein expressions of the TLR4/NF-kB signaling pathway were detected by the qRT-PCR and western blotting, respectively. *Results.* There were 53 ESI$^+$ and 50 ESI$^-$ components in PSR. After high-dose PSR treatment, $FEV_{0.3}$/FVC% and Cdyn increased significantly, while RI decreased. Compared with the COPD model, the RI of the Biostime Probiotic Powder group was significantly lower. HE staining showed that the inflammatory cell infiltration was reduced to varying degrees, the bronchial tube wall was not thickened, and the alveoli were relatively intact after treatment with PSR and Biostime Probiotic Powder. Compared with the model group, the levels of TNF-α, IFN-γ, IL-1β, IL-4, and IL-10 in the PSR group and the Biostime Probiotic Powder group were reversed. The mRNA and protein expressions of TLR4 and NF-kB were significantly decreased after PSR and Biostime Probiotic Powder treatment. *Conclusion.* Our findings suggest that PSR and Biostime Probiotic Powder have protective effects on COPD rats, which may be achieved by modulating the TLR4/NF-kB signaling pathway.

1. Introduction

Chronic obstructive pulmonary disease (COPD) is one of the leading causes of morbidity and mortality, characterized by persistent airflow limitation and increased chronic inflammatory response in lung tissue [1, 2]. It is widely accepted that the primary mechanism of COPD is chronic inflammation, including the release of inflammatory cytokines and immune cell responses [3]. Cigarette smoke and intratracheal administration of lipopolysaccharide (LPS) to rats are considered an ideal model of COPD. Previous studies have shown that cigarette smoke and LPS can stimulate airway epithelial cells to release harmful molecules that bind to toll-like receptor 4 (TLR4) on the cell surface [4, 5]. Activation of TLR4 induces nuclear factor kappa B

(NF-kB) and inflammatory cytokines, such as tumor necrosis factor alpha (TNF-α) [6, 7] and interleukin-1 beta(IL-1β) [8–10]. Therefore, the TLR4/NF-kB signaling pathway may play an important role in the pathogenesis of COPD.

It is reported that Chinese medicine has prominent advantages in the prevention and treatment of chronic diseases [11–18]. Peitu Shengjin Recipe (PSR) is a traditional Chinese herbal compound that varies slightly according to the patient's condition or individual differences. It has been reported that traditional Chinese medicine may be an alternative treatment method for COPD patients [19–21]. For example, BuzhongYiqi Decoction could improve lung function and sports ability [22], and Feikang granules could ameliorate pulmonary inflammation in COPD rats by the TLR2/4 mediated NF-kB pathway [4]. Gong et al. reported

that PSR could improve nutritional status and immune function in stable phase COPD patients [23]. In addition, the intestinal probiotics of COPD patients were significantly lower than that of healthy people [24]. Biostime Probiotic Powder has various functions, including promoting probiotic proliferation, inhibiting pathogenic bacteria, and enhancing metabolism and immune function [25, 26]. However, the effect and mechanism of Biostime Probiotic Powder on COPD have not been clearly studied.

In this study, we established a COPD rat model by exposure to cigarette smoke and intratracheal administration of LPS. PSR and Biostime Probiotic Powder were used to treat COPD rats. The effects of PSR and Biostime Probiotic Powder on COPD rats were evaluated by HE staining, ELISA, qRT-PCR, and western blotting.

2. Materials and Methods

2.1. Reagents. Paraxylene, absolute alcohol, citrate buffer, and phosphate buffer were purchased from SINOPHARM (Beijing, China). The enzyme-linked immunosorbent assay (ELISA) kits for TNF-α, IFN-γ, IL-1β, IL-4, and IL-10 were purchased from R&D Systems (Minneapolis, USA). The SYBR Green qPCR kit and reverse transcription kit were purchased from CWBIO (Beijing, China). The BCA protein assay kit and chemiluminescence detection reagent were purchased from Solarbio (Beijing, China). Anti-TLR4/MD2 complex (ab95562) and anti-NF-κB p65 (ab207297) were purchased from Abcam (Cambridge, USA). PSR decoction was prepared by the Ningbo City Hospital of Traditional Chinese Medicine. Biostime Probiotic Powder was purchased from BIOSTIME (Guangzhou, China).

2.2. UPLC-Q/TOF-MS Analysis. Chromatographic analysis was conducted on the Waters ACQUITY I-Class Plus UPLC system (Waters Corp., Milford, USA) and ACQUITY UPLC BEH C18 (100×2.1 mm, 1.7μm, AB SCIEX, Framingham, USA). The mobile phase was a mixture of acetonitrile with 0.1% formic acid and water with 0.1% formic acid. The gradient elution conditions were as follows: 0–2 min, 99% B; 2–12 min, 99%–55% B; 12 ∼ 19 min, 55%–1% B. MS spectrometry was performed on the SCIEX X-500R quadrupole time of flight mass spectrometer (AB SCIEX, Framingham, USA). The parameters were set as follows: ion source gas1 (Gas1):45, ion source gas2 (Gas2):55, curtain gas (CUR):35, source temperature: 600°C, ionSapary voltage floating (ISVF):5500 V/−4500 V; TOF MS scan m/z range: 100–1500 Da, production scan m/z range:25–1500 Da, TOF MS scan accumulation time: 0.25 s/spectra, and product ion scan accumulation time: 0.035 s/spectra. SCIEX OS software was used to collect and analyze data.

2.3. Animal and Group. Thirty male Sprague-Dawley (SD) rats, weighing 200 ± 20 g, were purchased from the Zhejiang Medical Laboratory Animal Center (Hangzhou, China). Fifty-five rats were randomly selected to replicate the COPD model through cigarette smoke combined with LPS. Rats were treated with 200 μl LPS (1 mg/ml) by gavage on days 1 and 14. From day 2 to day 28, rats were placed in a box and exposed to the smoke produced by a lighted cigarette for one hour per day. Carbon dioxide asphyxiation was performed before rats were dissected. The rats were divided into six groups: control group, model group, low, medium, and high-dose of the PSR group, and Biostime Probiotic Powder group. According to the dose conversion between adults and rats, the PSR-medium dose group was given 1.5 times the low dose, and the high-dose group was given three times the low dose. The rats in the normal group and the model group were given an equal volume of normal saline by oral gavage. Biostime Probiotic Powder was converted to rat dosage by gavage according to the instructions. All experiments were approved by the Animal Ethics Committee (EYOUNG-20201117-06), and this study was conducted in accordance with the National Institute of Health's Guideline for the Care and Use of Laboratory Animals.

2.4. Lung Function Assessment and HE Staining. After the last administration, lung function was measured by using an animal lung function analysis system (AniRes2005, Beijing, China). Rats were anesthetized, tracheostomized, and then connected to the instrument. $FEV_{0.3}$/FVC%, dynamic lung compliance (Cdyn), and resistance of inspiration (RI) were tested. Lung tissue was fixed with 4% paraformaldehyde and embedded in paraffin. Then, we used hematoxylin-eosin (HE) to stain sections (4μm thick). The light microscope was used to observe it.

2.5. ELISA. Blood samples were collected from the abdominal aorta and centrifuged at 3000 rpm/min for 15 min. According to the manufacturer's instructions, the levels of TNF-α, IFN-γ, IL-1β, IL-4, and IL-10 in the supernatant were determined using the ELISA kits (MEIMIAN, Jiangsu, China). The details of the ELISA were as follows: (1) We prepare and dilute reagents. (2) We set standard, sample, and control wells. 100 μl of the horseradish peroxidase-labeled antibody was added to the standard and sample wells. (3) The plate was incubated in a 37°C water bath for 60 min. (4) After washing, the chromogenic reagent was added to the plate for 15 min at 37°C. (5) The absorbance value was measured at 450 nm.

2.6. qRT-PCR. Total RNA was extracted from lung tissue with the Trizol reagent and reverse transcribed into cDNA. The reaction conditions were as follows: 15 min at 42°C and 5 min at 85°C. qRT-PCR was detected using the LightCycler ® 96 instrument (Roche, Basel, Switzerland), and the reaction conditions were as follows: denaturation at 95°C for 10 min; 15 s at 95°C; 60 s at 60°C (40 cycles). The primers were as follows: TLR4 (forward, AACTCTGCGCC-TAAAACCCA, reverse, TGCTACTTCCTTGTGCCCTG), NF-κB (forward, ACAGATTCTGGGGAGTGTGC, reverse, GAGCCGACTATCGTACAGGG), and GAPDH (forward, GATGGTGAAGGTCGGTGTGA, reverse, TGAACTTG-CCGTGGGTAGAG).

2.7. Western Blotting. Lung tissues were homogenized with lysis buffer and centrifuged at 4°C for 5 min, and the supernatant was taken. The total protein concentration of the samples was assayed using the BCA kits (Solarbio, Beijing, China). Samples were separated on 5% SDS-PAGE, transferred to PVDF membranes (GE Healthcare Life, Atlanta, USA), and blocked with 5% skim milk for 1.5 h. After 3 washes with TBST, the membrane was incubated overnight at 4°C with primary antibodies, including anti-TLR4/MD2 complex, anti-NF-κB p65, and anti-GAPDH (HUABIO, Hangzhou, China). Then, the membrane was washed with TBST three times. We incubated the membrane for 2 hours at room temperature using the appropriate horseradish peroxidase-conjugated secondary antibody. The enhanced chemiluminescence kit (Solarbio, Beijing, China) was utilized to visualize the membrane. At last, we used ImageJ software to calculate the relative protein levels.

2.8. Statistical Analysis. All values were expressed as the mean ± SD. GraphPad Prism software (Version 7.0, San Diego, USA) was used for statistical comparisons. The P value < 0.05 was regarded as statistically significant. For pairwise comparison between the groups, two independent samples t-test was used for homogeneous variances, and the Kruskal–Wallis H test was used for unequal variances.

3. Results

3.1. Components of Peitu Shengjin Recipe. The chemical composition of PSR was analyzed by UPLC-Q/TOF-MS in positive and negative ESI detection modes. The total ion flow diagram of PSR is shown in Figure 1. 53 and 50 components of PSR were identified by the positive and negative ion mode, respectively. It included amino acids, alkaloids, volatile oils, fatty acids, and other components, as given in Table 1 and Table 2.

3.2. Effects of Peitu Shengjin Recipe and Biostime Probiotic Powder on Lung Function. As shown in Table 3 and Figure 2, we measured $FEV_{0.3}$/FVC%, Cdyn, and RI to show the effect of PSR and Biostime Probiotic Powder on lung function. Compared with the controls, $FEV_{0.3}$/FVC% and Cdyn were significantly decreased, whereas RI was enhanced in the model group. After treatment of PSR and Biostime Probiotic Powder, there was no significant difference of $FEV_{0.3}$/FVC%, Cdyn, and RI in the PSR-low dose group and the PSR-medium dose group ($P > 0.05$). $FEV_{0.3}$/FVC% and Cdyn increased ($P < 0.05$), and RI significantly decreased ($P < 0.01$) in the PSR-high dose group. There were no remarkable changes in $FEV_{0.3}$/FVC% and Cdyn, but RI values in the Biostime Probiotic Powder group were statistically different. In addition, we stained lung tissues of the six groups with HE (Table 4 and Figure 3). In the controls, the bronchus was intact and the mucosa was not shedding, and there was no inflammatory cell infiltration. In the model group, the bronchus was broken incompletely, the trachea was shrunk, the lumen was narrowed, the tracheal mucosa was detached, and a large number of inflammatory cells were infiltrated around. The tracheal mucosa was intact in the low, medium, and high-dose groups of PSR, and the peripheral inflammatory cell infiltration was less than that in the model group. The Biostime Probiotic Powder group also had a protective effect on lung tissue.

3.3. Effects of Peitu Shengjin Recipe and Biostime Probiotic Powder on Inflammatory Factors. TNF-α, IFN-γ, IL-1β, IL-4, and IL-10 in serum were measured by the ELISA. As shown in Figure 4, the serum levels of TNF-α, IFN-γ, and IL-1β in the model group were significantly higher than those in the control group, and IL-4 and IL-10 levels were significantly decreased ($P < 0.01$). Compared with the model group, IFN-γ levels obviously decreased in the PSR-low dose group; TNF-α and IFN-γ levels significantly decreased in the PSR-medium dose group; the serum levels of TNF-α, IFN-γ, and IL-1β significantly decreased in the PSR-high dose group, whereas IL-4 and IL-10 increased ($P < 0.01$). In the Biostime Probiotic Powder group, the levels of TNF-α and IFN-γ were decreased, the levels of IL-4 were increased, and the levels of IL-1β and IL-10 had no significant changes.

3.4. Effects on Peitu Shengjin Recipe and Biostime Probiotic Powder on the TLR4/NF-kB Pathway. Figure 5(a) shows that the mRNA level of TLR4 in the PSR-high dose group was significantly decreased compared with that of the COPD model group. After treatment with high-dose PSR and Biostime Probiotic Powder, NF-kB expression was significantly increased ($P < 0.05$). Meanwhile, we performed the western blotting to detect the protein levels of TLR4 and NF-kB p65 (Figure 5(b)). The results showed that the expression level of TLR4 protein in the PSR-medium dose group was significantly decreased ($P < 0.05$). The levels of TLR4 and NF-kB p65 in the lung tissue of rats in the PSR-medium dose group and the Biostime Probiotic Powder group were significantly decreased ($P < 0.01$).

4. Discussion

In this study, we identified the chemical composition of PSR. The therapeutic effects of PSR and Biostime Probiotic Powder on COPD rats were also explored. Our results showed that PSR and Biostime Probiotic Powder attenuated airway inflammation in COPD rats by downregulating the TLR4/NF-kB signaling pathway.

COPD will be the third leading cause of death by 2030 [27]. The current pharmacological treatments include bronchodilators and antibiotics combined with corticosteroids, which could not cure COPD [28, 29]. Inhibition of TLRs has been reported to be a key cellular target for initiating and sustaining inflammation and improving lung function and thus playing a therapeutic role in COPD patients [30]. TLR4 is the first identified mammalian TLR, expressed in inflammatory cells. In lung tissue, TLR4 may be activated by risk factors such as smoking, inhalation of contaminated air, and bacterial and viral infections, which in turn activate NF-kB and induce the expression of inflammatory mediators [31]. In the study, we established the
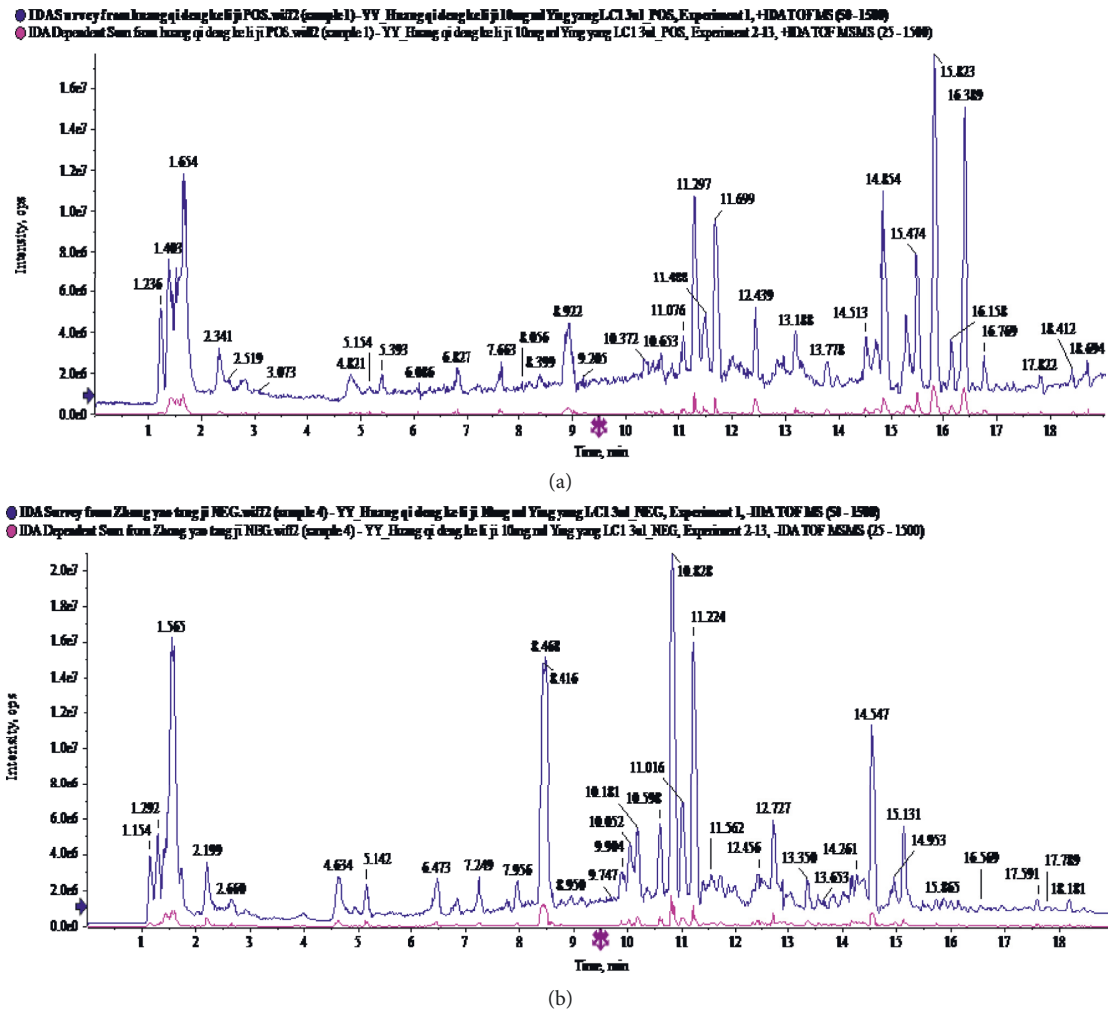
(a)

(b)

Figure 1: The total ion flow diagram of Peitu Shengjin Recipe by UPLC-Q/TOF-MS. (a) Positive mode. (b) Negative mode.

Table 1: The chemical components of Peitu Shengjin Recipe in the positive mode.

NO.	Component name	Area	Retention time	Formula	Precursor mass	Found at mass	Mass error (ppm)	Library score	Isotope ratio difference
1	Histidine	$1.98E + 05$	1.39	$C_6H_9N_3O_2$	156.077	156.0768	0.5	95.4	0.7
2	L(+)-Arginine	$8.20E + 06$	1.4	$C_6H_{14}N_4O_2$	175.119	175.1188	−1.1	80	0.9
3	Threonine	$3.61E + 05$	1.47	$C_4H_9NO_3$	120.066	120.0654	−1.0	86.6	1.1
4	Glutamic acid	$4.45E + 05$	1.51	$C_5H_9NO_4$	148.06	148.0604	−0.3	96.9	0.7
5	Betaine	$5.75E + 05$	1.52	$C_5H_{11}NO_2$	118.086	118.0862	−0.4	100	0.1
6	Sorbitol	$3.08E + 05$	1.53	$C_6H_{14}O_6$	183.086	183.0863	0	93.3	0.6
7	Trigonelline	$1.51E + 06$	1.59	$C_7H_7NO_2$	138.055	138.0547	−1.9	95.9	0.8
8	Proline	$4.67E + 06$	1.62	$C_5H_9NO_2$	116.071	116.0704	−1.9	99.2	0.8
10	Adenine	$7.04E + 05$	1.67	$C_5H_5N_5$	136.062	136.0616	−1.1	89	1.8
9	Stachydrine	$9.68E + 06$	1.67	$C_7H_{13}NO_2$	144.102	144.1016	−1.8	100	0.2
11	Nicotinic acid	$2.74E + 05$	2.36	$C_6H_5NO_2$	124.039	124.0393	−0.3	95.4	0.2
12	Nicotinamide	$1.66E + 05$	2.52	$C_6H_6N_2O$	123.055	123.0552	−0.5	97.8	1.7
13	6-Hydroxypurine	$8.76E + 04$	2.66	$C_5H_4N_4O$	137.046	137.0458	−0.3	75	1
14	Adenosine	$1.16E + 06$	4.95	$C_{10}H_{13}N_5O_4$	268.104	268.1038	−0.7	100	0.9
15	Guanosine	$2.38E + 05$	5.18	$C_{10}H_{13}N_5O_5$	284.099	284.0992	1.0	100	0.8
16	Phenylalanine	$6.42E + 05$	6.09	$C_9H_{11}NO_2$	166.086	166.0862	−0.6	98.3	1.1
17	Esculin hydrate	$3.71E + 04$	7.84	$C_{15}H_{16}O_9$	341.087	341.0874	2.1	75.5	1.3

Table 1: Continued.

NO.	Component name	Area	Retention time	Formula	Precursor mass	Found at mass	Mass error (ppm)	Library score	Isotope ratio difference
18	Chlorogenic acid	$1.59E + 05$	8.39	$C_{16}H_{18}O_9$	355.102	355.1025	0.5	99.1	1.1
19	Cryptochlorogenic acid	$1.59E + 05$	8.39	$C_{16}H_{18}O_9$	355.102	355.1025	0.5	99.1	1.1
20	Typhaneoside	$2.48E + 04$	9.43	$C_{34}H_{42}O_20$	771.234	771.2348	0.7	78.8	3
21	Schaftoside	$2.67E + 05$	9.58	$C_{26}H_{28}O_{14}$	565.155	565.1557	1.0	97.6	2.3
22	Calycosin-7-O-glucoside	$2.54E + 06$	10.45	$C_{22}H_{22}O_{10}$	447.129	447.1283	−0.5	100	0.3
23	Eriodictyol	$5.46E + 05$	10.59	$C_{15}H_{12}O_6$	289.071	289.0707	0.2	93.4	1.3
24	PolygalaxanthoneIV	$6.77E + 05$	10.59	$C_{27}H_{32}O_{15}$	597.181	597.1818	0.6	90.8	2.4
25	Isoliquiritigenin	$3.94E + 06$	10.67	$C_{15}H_{12}O_4$	257.081	257.0806	−1.0	92.2	0.7
26	7-Hydroxycoumarin	$3.82E + 05$	10.85	$C_9H_6O_3$	163.039	163.0389	−0.2	86.5	0.2
27	Isoferulic acid	$2.11E + 05$	10.9	$C_{10}H_{10}O_4$	195.065	195.0651	−0.4	97.2	1.2
28	Naringenin	$9.48E + 06$	11.3	$C_{15}H_{12}O_5$	273.076	273.0757	−0.2	100	0.5
29	Narirutin	$9.62E + 06$	11.3	$C_{27}H_{32}O_{14}$	581.186	581.1867	0.4	90.3	3.6
30	Hesperetin	$7.56E + 06$	11.7	$C_{16}H_{14}O_6$	303.086	303.0864	0.3	100	1.4
31	Hesperidin	$1.08E + 07$	11.7	$C_{28}H_{34}O_{15}$	611.197	611.197	0	92.2	1.3
32	Apigenin 7-O-beta-D-glucuronide	$6.53E + 04$	12.35	$C_{21}H_{18}O_{11}$	447.092	447.093	1.8	95	0.5
33	Ononin	$1.81E + 06$	12.47	$C_{22}H_{22}O_9$	431.134	431.134	0.8	98.6	0.5
34	Methylhesperidin	$5.94E + 04$	12.48	$C_{29}H_{36}O_{15}$	625.213	625.2127	0	93.9	4.7
35	6,7-Dimethoxycoumarin	$5.10E + 04$	12.51	$C_{11}H_{10}O_4$	207.065	207.0652	0.2	87.8	2.5
36	Isomucronulatol	$9.71E + 04$	13.11	$C_{17}H_{18}O_5$	303.123	303.1229	0.6	96.5	1.7
37	Xanthotoxol	$1.38E + 05$	13.32	$C_{11}H_6O_4$	203.034	203.034	0.3	76.3	2.1
38	Wogonin 7-O-glucuronide	$2.61E + 04$	13.52	$C_{22}H_{20}O_{11}$	461.108	461.1083	1.1	100	4.2
39	Tectorigenin	$1.12E + 05$	14.02	$C_{16}H_{12}O_6$	301.071	301.0707	0	82.1	0.1
40	AstragalosideIV	$1.07E + 05$	14.68	$C_{41}H_{68}O_{14}$	785.468	785.4687	0.7	92.3	3.2
41	Glycyrrhizic acid	$9.83E + 06$	14.85	$CVH_{62}O_{16}$	823.411	823.4109	−0.2	96.7	3.7
42	Formononetin	$1.31E + 06$	15.1	$C_{16}H_{12}O_4$	269.081	269.0806	−1.0	99.6	0.9
43	Limonin	$6.50E + 06$	15.48	$C_{26}H_{30}O_8$	471.201	471.2015	0.4	91.4	1.6
44	Isovanillin	$7.98E + 04$	15.51	$C_8H_8O_3$	153.055	153.0546	0	92.1	1.3
45	Nobiletin	$4.66E + 07$	15.82	$C_{21}H_{22}O_8$	403.139	403.1382	−1.4	98	0.5
46	Tangeretin	$3.52E + 07$	16.39	$C_{20}H_{20}O_7$	373.128	373.1276	−1.5	98.4	0.2
47	Parthenolide	$5.82E + 04$	16.56	$C_{15}H_{20}O_3$	249.149	249.1485	−0.2	80.6	2
48	3-N-butyl-4,5-dihydrophthalide	$8.80E + 04$	16.56	$C_{12}H_{16}O_2$	193.122	193.1222	−0.8	90.7	2
49	Glabridin	$2.34E + 04$	17.04	$C_{20}H_{20}O_4$	325.143	325.1437	0.7	97.8	3.1
50	Osthole	$9.77E + 04$	17.33	$C_{15}H_{16}O_3$	245.117	245.1172	0.1	91.7	1.1
51	Anisaldehyde	$1.76E + 05$	17.59	$C_8H_8O_2$	137.06	137.0596	-0.8	95.4	0.5
52	Isoalantolactone	$1.57E + 05$	17.65	$C_{15}H_{20}O_2$	233.154	233.1537	0.3	95.6	1.7
53	Patchouli alcohol (loss H_2O)	$1.26E + 04$	19.31	$C_{15}H_{24}$	205.195	205.195	−0.5	90.7	1.7

Table 2: The chemical components of Peitu Shengjin Recipe in the negative mode.

NO.	Component name	Area	Retention time	Formula	Precursor mass	Found at mass	Mass error (ppm)	Library score	Isotope ratio difference
1	L(+)-Arginine	$8.54E + 05$	1.3	$C_6H_{14}N_4O_2$	173.104	173.1046	1.0	98.7	1.4
2	Histidine	$1.12E + 05$	1.3	$C_6H_9N_3O_2$	154.062	154.0623	0.8	91.7	0.8
3	Aspartic acid	$3.76E + 05$	1.37	$C_4H_7NO_4$	132.03	132.0304	0.9	88.3	0.6
4	Glutamic acid	$7.10E + 04$	1.38	$C_5H_9NO_4$	146.046	146.046	0.8	98.2	1.4
5	Sorbitol	$2.51E + 05$	1.42	$C_6H_{14}O_6$	181.072	181.0721	1.8	85	0.8
6	D-(+)-Mannose	$1.07E + 06$	1.52	$C_6H_{12}O_6$	179.056	179.0563	0.9	80.1	0.6
7	Quinic acid	$2.43E + 06$	1.54	$C_7H_{12}O_6$	191.056	191.0563	1.0	89.3	0.5
8	Maltopentaose	$9.00E + 05$	1.59	$C_{30}H_{52}O_{26}$	827.267	827.2686	1.5	96.1	2.4
9	Maleic acid	$7.19E + 05$	1.63	$C_4H_4O_4$	115.004	115.0037	0.4	99.6	0.3

TABLE 2: Continued.

NO.	Component name	Area	Retention time	Formula	Precursor mass	Found at mass	Mass error (ppm)	Library score	Isotope ratio difference
10	Citric acid	$4.43E + 06$	2.66	$C_6H_8O_7$	191.02	191.0201	1.9	99.1	0.6
11	Guanosine	$3.39E + 05$	4.94	$C_{10}H_{13}N_5O_5$	282.084	282.0848	1.6	99.6	0.2
12	Phenprobamate	$1.73E + 05$	5.77	$C_9H_{11}NO_2$	164.072	164.0718	0.9	96.1	0.6
13	Protocatechuic acid	$6.14E + 04$	6.49	$C_7H_6O_4$	153.019	153.0193	-0.1	93.7	1.8
14	L-Tryptophan	$3.43E + 05$	7.23	$C_{11}H_{12}N_2O_2$	203.083	203.0828	0.9	97.2	0.5
15	Protocatechuic aldehyde	$5.79E + 04$	7.78	$C_7H_6O_3$	137.024	137.0245	0.8	96.7	0.9
16	Caffeic acid	$1.55E + 05$	8.61	$C_9H_8O_4$	179.035	179.035	0.3	91.6	0.7
17	Troxerutin +HCOOH	$2.52E + 05$	9.14	$C_{33}H_{42}O_{19}.HCOOH$	787.23	787.2313	1.3	99.1	2.4
18	Daidzin	$8.91E + 04$	9.53	$C_{21}H_{20}O_9$	415.103	415.1038	0.8	96.3	2.3
19	p-Coumaric acid	$1.03E + 05$	9.87	$C_9H_8O_3$	163.04	163.0401	0.5	97.7	1.1
20	Calycosin-7-o-glucoside +HCOOH	$1.67E + 06$	9.96	$C_{22}H_{22}O_{10}.HCOOH$	491.119	491.1203	1.6	99.6	1.4
21	Neoeriocitrin	$4.08E + 06$	10.12	$C_{27}H_{32}O_{15}$	595.167	595.1677	1.5	98.6	2.7
22	Liquiritin	$1.08E + 07$	10.19	$C_{21}H_{22}O_9$	417.119	417.1199	1.9	98.8	1.6
23	7-Hydroxycoumarin	$5.37E + 05$	10.33	$C_9H_6O_3$	161.024	161.0246	1.2	96.6	0.1
24	Isoferulic acid	$4.83E + 05$	10.39	$C_{10}H_{10}O_4$	193.051	193.0508	0.8	98.4	0.5
25	Isochlorogenic acid B	$3.49E + 05$	11.02	$C_{25}H_{24}O_{12}$	515.119	515.12	1.0	99.8	2.2
26	Apigenin 7-O-beta-D-glucuronide	$6.94E + 04$	11.88	$C_{21}H_{18}O_{11}$	445.078	445.0779	0.6	88.9	1.7
27	Ononin +HCOOH	$1.75E + 06$	11.99	$C_{22}H_{22}O_9.HCOOH$	475.125	475.1251	1.0	99.5	2.3
28	Methylhesperidin	$6.58E + 04$	12.01	$C_{29}H_{36}O_{15}$	623.198	623.1988	1.1	89	2.2
29	Platycodin D	$6.42E + 05$	12.43	$C_{57}H_{92}O_{28}$	1223.57	1223.5716	1.1	92.4	4.5
30	Isoliquiritigenin	$9.56E + 05$	12.49	$C_{15}H_{12}O_4$	255.066	255.0665	1.0	92.7	1
31	Pterostilbene	$4.85E + 03$	12.5	$C_{16}H_{16}O_3$	255.103	255.1027	-0.1	92.7	2.1
32	Eriodictyol	$4.30E + 04$	12.58	$C_{15}H_{12}O_6$	287.056	287.0564	0.9	96.9	2
33	Isomucronulatol-7-O-glucoside	$4.20E + 05$	12.64	$C_{23}H_{28}O_{10}$	463.161	463.1616	1.4	98.5	1.5
34	Calycosin	$8.26E + 05$	12.7	$C_{16}H_{12}O_5$	283.061	283.0616	1.3	98.9	0.9
35	Xanthotoxol	$3.82E + 05$	12.81	$C_{11}H_6O_4$	201.019	201.0196	1.4	91.1	0.7
36	Wogonin 7-O-glucuronide	$2.63E + 04$	13.06	$C_{22}H_{20}O_{11}$	459.093	459.0937	0.8	97.3	2.3
37	Naringenin	$1.33E + 06$	13.67	$C_{15}H_{12}O_5$	271.061	271.0615	1.2	100	0.8
38	Isorhamnetin	$4.21E + 04$	13.97	$C_{16}H_{12}O_7$	315.051	315.0513	0.9	86.9	1.7
39	Hesperetin	$6.93E + 05$	14.02	$C_{16}H_{14}O_6$	301.072	301.0721	1.0	94.5	2.8
40	Formononetin	$7.94E + 05$	14.72	$C_{16}H_{12}O_4$	267.066	267.0666	1.3	99.2	0.8
41	Pectolinarigenin	$1.52E + 05$	15.18	$C_{17}H_{14}O_6$	313.072	313.072	0.9	98.4	4.5
42	Eupatilin	$1.34E + 05$	15.42	$C_{18}H_{16}O_7$	343.082	343.0827	1.0	92.9	1.5
43	Obacunone	$4.44E + 04$	15.56	$C_{26}H_{30}O_7$	453.192	453.1923	0.9	100	3.8
44	Chrysosplenetin B	$5.12E + 05$	15.59	$C_{19}H_{18}O_8$	373.093	373.0932	0.8	93.9	0.1
45	Astragaloside I +HCOOH	$8.18E + 05$	16.15	$C_{45}H_{72}O_{16}.HCOOH$	913.48	913.4807	0.5	99.8	2.6
46	Glabridin	$4.18E + 04$	16.78	$C_{20}H_{20}O_4$	323.129	323.1289	-0.1	91.5	0.7
47	Ginsenoside-Ro	$2.00E + 05$	17.18	$C_{48}H_{76}O_{19}$	955.491	955.4911	0.3	87.9	3.5
48	Gingerglycolipid B +HCOOH	$1.30E + 05$	17.48	$C_{33}H_{58}O_{14}.HCOOH$	723.381	723.3811	0.4	96.3	1.6
49	Glycyrrhetinic acid	$5.68E + 04$	18.35	$C_{30}H_{46}O_4$	469.332	469.3325	0.3	100	1.4
50	Pachymic acid	$1.47E + 05$	19.46	$C_{33}H_{52}O_5$	527.374	527.3745	0.5	100	0.6

COPD model in rats by combining smoking and LPS. The results of lung function assessment and HE staining showed the damages of lung tissue in COPD rats. In addition, the ELISA assay indicated that the COPD model induced the release of TNF-α, IFN-γ, and IL-1β and decreased levels of IL-4 and IL-10. This finding is consistent with a previous research study. Alexander et al. observed an increase of TNF-α and IL-1β in bronchoalveolar lavage of long-term smokers [32]. Wang et al. reported that LPS enhanced the expression of IFN-γ in rat pulmonary artery smooth muscle cells through the TLR4/IRAK/NF-kB pathway [31]. Moreover, Gu et al. showed a significant decrease in serum IL-4 and IL-10 concentrations [33].

Medicinal plants have been reported to have many biological effects [34–41]. In China, PSR has been shown to have clinical efficacy in the treatment of COPD patients [23, 42, 43]. PSR is composed of Astragalus, Codonopsis, Angelica, Atractylodes, Fructus aurantii, peach kernel,

TABLE 3: The pulmonary function assessment in rats with COPD.

Group	FEV0.3/FVC (%)	Cdyn (mL/cmH$_2$O)	RI (cmH$_2$O/mL/s)
Control	88.96 ± 8.83	0.50 ± 0.06	0.11 ± 0.03
Model	58.64 ± 4.12▲▲	0.33 ± 0.04▲	0.21 ± 0.03▲▲
PSR-low dose	62.94 ± 5.18	0.37 ± 0.04	0.19 ± 0.02
PSR-medium dose	70.04 ± 6.54	0.40 ± 0.05	0.16 ± 0.03
PSR-high dose	72.52 ± 7.02★	0.42 ± 0.04★	0.12 ± 0.02★★
Biostime Probiotic Powder	64.65 ± 6.30	0.41 ± 0.05	0.14 ± 0.02★

COPD: chronic obstructive pulmonary disease; Cdyn: dynamic lung compliance; RI: resistance of inspiration; PSR: Peitu Shengjin Recipe. ▲$P < 0.05$ and ▲▲$P < 0.01$ vs. the control group; ★$P < 0.05$ and ★★$P < 0.01$ vs. the model group.
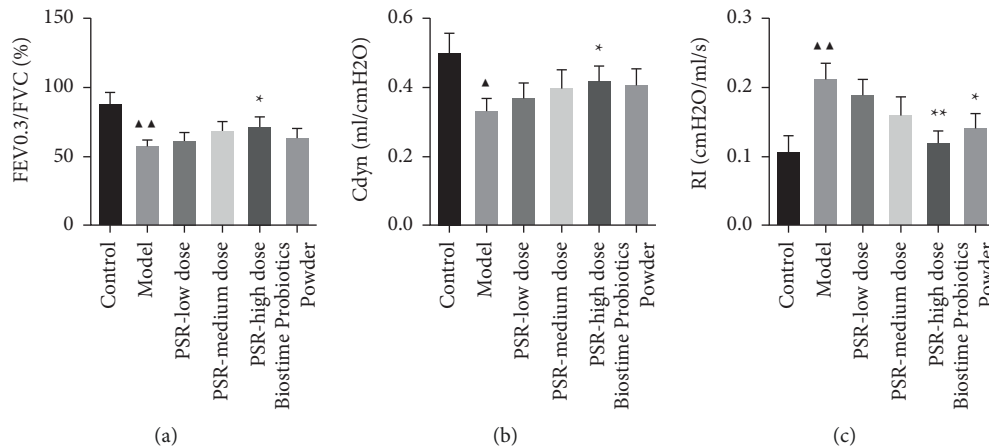

FIGURE 2: Peitu Shengjin Recipe and Biostime Probiotic Powder improved the lung function of rats with COPD. (a) FEV0.3/FVC (%). (b) Dynamic lung compliance (Cdyn). (c) Resistance of inspiration (RI). *Note*: ▲$P < 0.05$ and ▲▲$P < 0.01$ vs. the control group; ★$P < 0.05$ and ★★$P < 0.01$ vs. the model group.

TABLE 4: Semiquantitative evaluation of HE in lung tissue of rats with COPD.

Group	Semiquantitative score
Control	–
Model	3.67 ± 0.58
PSR-low dose	3.33 ± 0.58▲
PSR-medium dose	2.33 ± 0.58▲
PSR-high dose	1.67 ± 0.58▲
Biostime Probiotic Powder	1.33 ± 0.58▲▲

COPD: chronic obstructive pulmonary disease; PSR: Peitu Shengjin Recipe. ▲$P < 0.05$ and ▲▲$P < 0.01$ vs. the model group.

tangerine peel, Poria cocos, Pinellia ginger, Platycodon grandiflorum, and licorice [44]. PSR has the effect of invigorating the spleen and nourishing the lung. Our results showed that the components of PSR included nobiletin, isoliquiritigenin, 7-hydroxycoumarin, caffeic acid, and so on. Nobiletin has been reported to exhibit anti-inflammatory, anticancer, and anti-insulin resistance activities. Li et al. found that nobiletin has a protective effect on lung injury by inhibiting NF-kB activation [22]. Isoliquiritigenin also possesses antioxidative and anti-inflammatory properties by inhibiting the NF-kB and NLRP3 pathways [23]. Jose et al. found that 7-hydroxycoumarin has effects on the apoptosis and the cell cycle of human lung cancer cells [23]. Meanwhile, caffeic acid was found to have anti-inflammatory and ameliorative effects against tobacco smoking on the lung, heart, and kidney [45]. The underlying mechanism of PSR on COPD might be related to nobiletin, isoliquiritigenin, and other components. Therefore, we explored the mechanisms of different doses of PSR in COPD rats. The ELISA showed that PSR significantly affected the levels of TNF-α, IFN-γ, IL-1β, IL-4, and IL-10 in a dose-dependent manner. In the TLR4/NF-kB signaling pathway, high-dose PSR could significantly downregulate the expression of TLR4 and NF-kB. This suggests PSR may improve inflammatory status in the lung, and the effect is dose-dependent. It provided a theoretical basis for further clinical application of PSR. At the same time, we assessed the effects of Biostime Probiotic Powder on COPD rats. It also has a therapeutic effect on COPD but is not superior to high-dose PSR. The results indicated that Biostime Probiotic Powder significantly decreased the levels of TNF-α and IFN-γ and increased the concentration of IL-4 in serum. The western blotting and qRT-PCR showed that Biostime Probiotic Powder significantly reduced the expression of NF-kB. It is suggested that Biostime Probiotic Powder could play a vital role in the treatment of COPD by regulating inflammatory cytokines through the TLR4/NF-kB signaling pathway. In clinic, Biostime Probiotic Powder might be used to cure COPD.
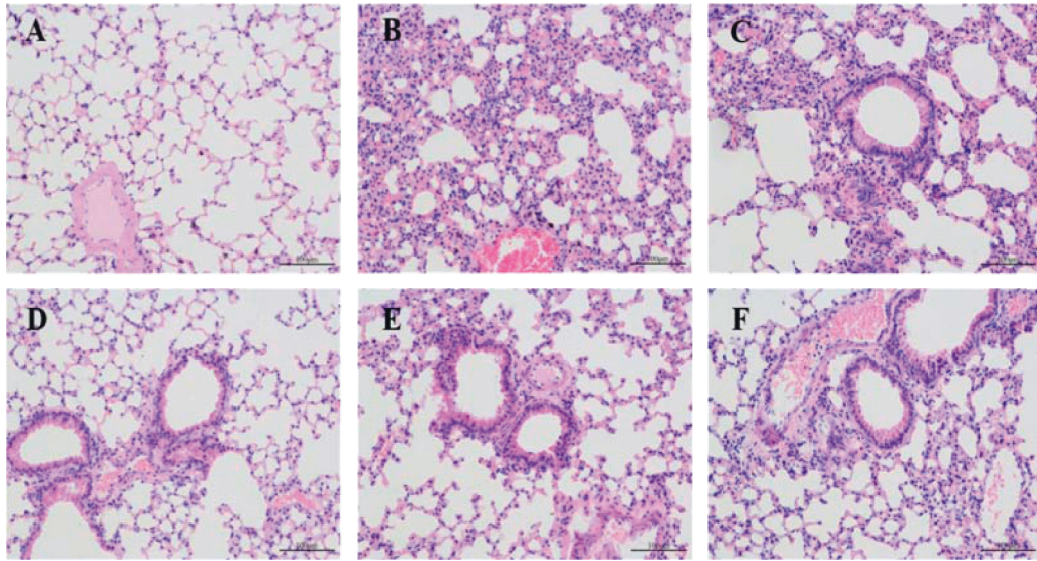
FIGURE 3: The effects of Peitu Shengjin Recipe and Biostime Probiotic Powder on lung tissue. (a) Control group. (b) Model group. (c) PSR-low dose group. (d) PSR-medium dose group. (e) PSR-high dose group. (f) Biostime Probiotic Powder group.
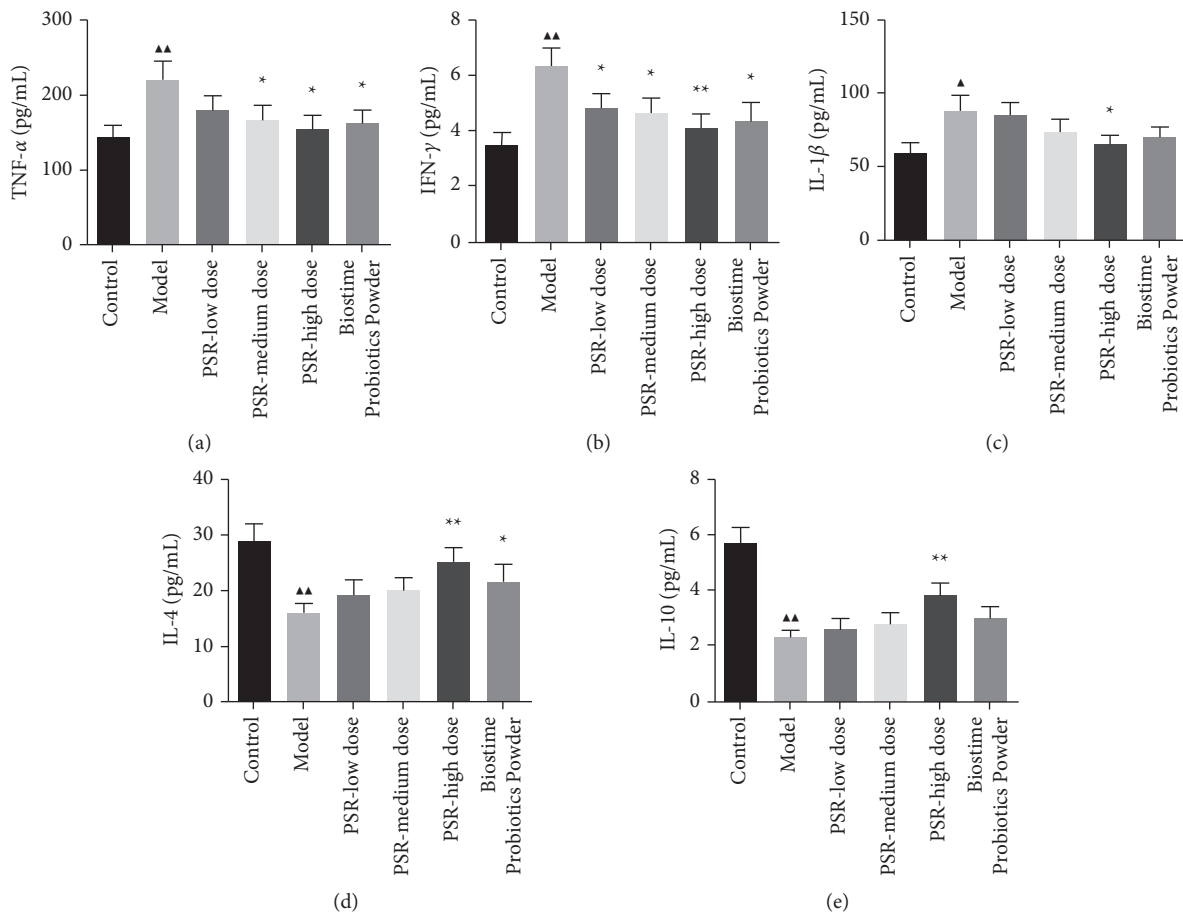

FIGURE 4: Serum levels of TNF-α, IFN-γ, IL-1β, IL-4, and IL-10 in rats. *Note*: $^{\blacktriangle}P < 0.05$ and $^{\blacktriangle\blacktriangle}P < 0.01$ vs. the control group; $P < 0.05$ and $P < 0.01$ vs. the model group.
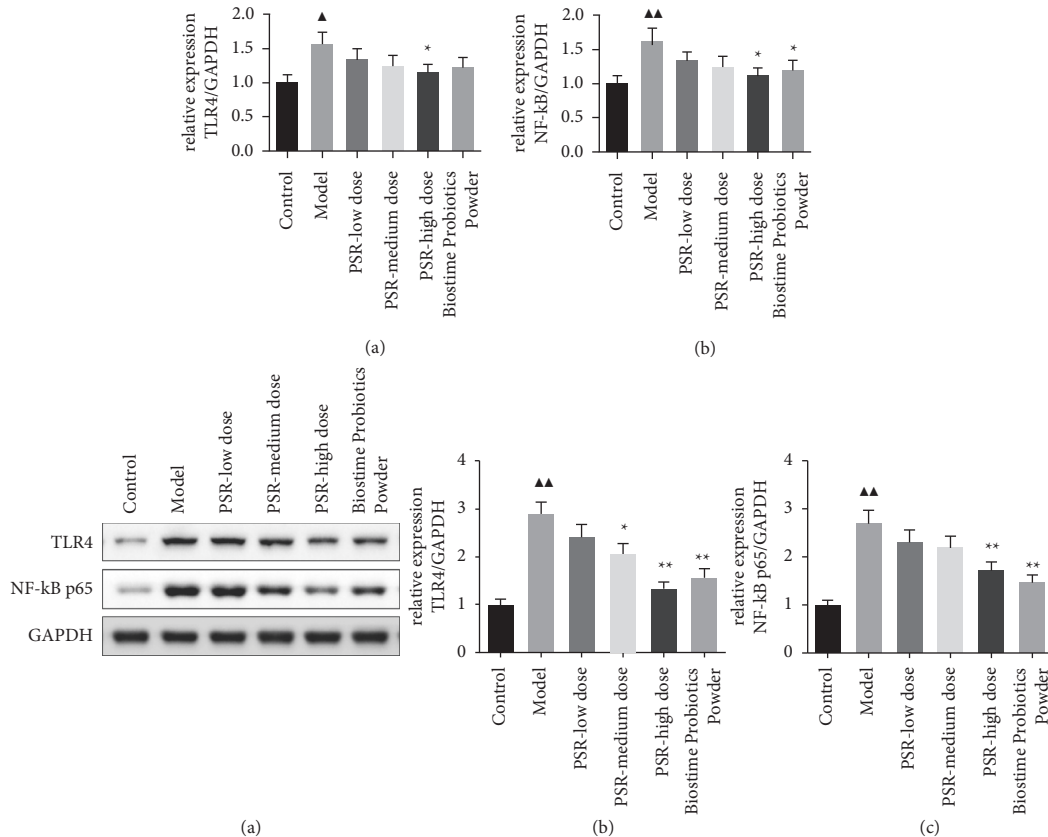
Figure 5: The expressions of TLR4 and NF-kB p65 in lung tissue. (a) mRNA levels; (b) protein levels. *Note*: ▲$P < 0.05$ and ▲▲$P < 0.01$ vs. the control group; $P < 0.05$ and $P < 0.01$ vs. the model group.

In conclusion, our results demonstrated that PSR and Biostime Probiotic Powder had a protective effect against COPD. PSR and Biostime Probiotic Powder could improve lung function, reverse the levels of inflammation-related cytokines, and regulate the mRNA and protein expressions of the TLR4/NF-kB signaling pathway. The therapeutic effect of PSR and Biostime Probiotic Powder was attributed to the inhabitation of the TLR4/NF-kB signaling pathway. Hence, our study showed that PSR and Biostime Probiotic Powder are promising therapeutic targets for COPD.

Data Availability

All data are available in our study.

Conflicts of Interest

The authors declare that they have no conflicts of interest.

Acknowledgments

References

[1] Y. Tang, Q. H. Cai, Y. J. Wang et al., "Protective effect of autophagy on endoplasmic reticulum stress induced apoptosis of alveolar epithelial cells in rat models of COPD," *Bioscience Reports*, vol. 37, no. 6, 2017.

[2] P. Zhang, X. Xin, L. Fang et al., "HMGB1 mediates *Aspergillus fumigatus*-induced inflammatory response in alveolar macrophages of COPD mice via activating MyD88/NF-κB and syk/PI3K signalings," *International Immunopharmacology*, vol. 53, pp. 125–132, 2017.

[3] P. J. Barnes, "Targeting cytokines to treat asthma and chronic obstructive pulmonary disease," *Nature Reviews Immunology*, vol. 18, no. 7, pp. 454–466, 2018.

[4] L. Yang, M. Wen, X. Liu, K. Wang, and Y. Wang, "Feikang granules ameliorate pulmonary inflammation in the rat model of chronic obstructive pulmonary disease via TLR2/4-mediated NF-κB pathway," *BMC Complementary Medicine and Therapies*, vol. 20, 2020.

[5] Z. Li, X. Xiao, and M. Yang, "Asiatic acid inhibits lipopolysaccharide-induced acute lung injury in mice," *Inflammation*, vol. 39, no. 5, pp. 1642–1648, 2016.

[6] S. H. Park, H. J. Choi, S. Y. Lee, and J. S. Han, "TLR4-mediated IRAK1 activation induces TNF-α expression via JNK-dependent NF-κB activation in human bronchial epithelial cells," *European Journal of Inflammation*, vol. 13, no. 3, pp. 183–195, 2015.

[7] A. K. Yi, J. G. Yoon, S. C. Hong, T. W. Redford, and A. M. Krieg, "Lipopolysaccharide and CpG DNA synergize for tumor necrosis factor-α production through activation of NF-κB," *International Immunology*, vol. 13, no. 11, pp. 1391–1404, 2001.

[8] J. L. Yu, X. S. Zhang, X. Xue, and R. M. Wang, "Patchouli alcohol protects against lipopolysaccharide-induced acute lung injury in mice," *Journal of Surgical Research*, vol. 194, no. 2, pp. 537–543, 2015.

[9] Y. L. Liu, Y. J. Liu, Y. Liu et al., "Hydroxy safflor yellow A ameliorates lipopolysaccharide-induced acute lung injury in mice via modulating toll-like receptor 4 signaling pathways," *International Immunopharmacology*, vol. 23, no. 2, pp. 649–657, 2014.

[10] Y. Guan, J. Q. Chen, X. Y. Li, and S. N. Jiang, "ClyA enhances LPS-induced IL-1β secretion in human macrophages through TLR4 and NLRP3 signaling," *Journal of Biological Regulators & Homeostatic Agents*, vol. 35, no. 2, pp. 495–504, 2021.

[11] P. Tagde, P. Tagde, F. Islam et al., "The multifaceted role of curcumin in advanced nanocurcumin form in the treatment and management of chronic disorders," *Molecules*, vol. 26, no. 23, p. 7109, 2021.

[12] F. Islam, S. Bibi, A. F. K. Meem et al., "Natural bioactive molecules: an alternative approach to the treatment and control of COVID-19," *International Journal of Molecular Sciences*, vol. 22, 2021.

[13] A. Akter, F. Islam, S. Bepary et al., "CNS depressant activities ofAverrhoa carambola leaves extract in thiopental-sodium model of Swiss albino mice: implication for neuro-modulatory properties," *Biologia*, vol. 77, no. 5, pp. 1337–1346, 2022.

[14] F. Islam, S. Mitra, M. H. Nafady et al., "Neuropharmacological and antidiabetic potential of lannea coromandelica (houtt.) merr. Leaves extract: an experimental analysis," *Evidence-based Complementary and Alternative Medicine*, vol. 2022, Article ID 6144733, 1–10 pages, 2022.

[15] F. Islam, S. Shohag, M. J. Uddin et al., "Exploring the journey of zinc oxide nanoparticles (ZnO-NPs) toward biomedical applications," *Materials*, vol. 15, no. 6, 2022.

[16] M. R. Islam, F. Islam, M. H. Nafady et al., "Natural small molecules in breast cancer treatment: understandings from a therapeutic viewpoint," *Molecules*, vol. 27, no. 7, 2022.

[17] M. M. Rahman, F. Islam, A. Parvez et al., "Citrus limon L. (lemon) seed extract shows neuro-modulatory activity in an in vivo thiopental-sodium sleep model by reducing the sleep onset and enhancing the sleep duration," *Journal of Integrative Neuroscience*, vol. 21, no. 1, 2022.

[18] S. Mitra, M. S. Lami, A. Ghosh et al., "Hormonal therapy for gynecological cancers: how far has science progressed toward clinical applications?" *Cancers*, vol. 14, no. 3, 2022.

[19] F. Roviezzo, A. Rossi, E. Caiazzo et al., "Palmitoylethanolamide supplementation during sensitization prevents airway allergic symptoms in the mouse," *Frontiers in Pharmacology*, vol. 8, 2017.

[20] A. Rossi, E. Caiazzo, R. Bilancia et al., "Salvinorin A inhibits airway hyperreactivity induced by ovalbumin sensitization," *Frontiers in Pharmacology*, vol. 7, 2016.

[21] M. A. R. B. Shovo, M. R. Tona, J. Mouah et al., "Computational and pharmacological studies on the antioxidant, thrombolytic, anti-inflammatory, and analgesic activity of molineria capitulata," *Current Issues in Molecular Biology*, vol. 43, no. 2, pp. 434–456, 2021.

[22] L. Wu, Y. Chen, Y. Xu, X. Li et al., "Oral huangqi formulae for stable chronic obstructive pulmonary disease: a systematic review and meta-analysis," *Evidence Based Complementary & Alternative Medicine*, vol. 2013, Article ID 705315, 14 pages, 2013.

[23] J. S. Lopez-Gonzalez, H. Prado-Garcia, D. Aguilar-Cazares, J. A. Molina-Guarneros, J. Morales-Fuentes, and J. J. Mandoki, "Apoptosis and cell cycle disturbances induced by coumarin and 7-hydroxycoumarin on human lung carcinoma cell lines," *Lung Cancer*, vol. 43, no. 3, pp. 275–283, 2004.

[24] M. Warren, M. S. Mccarthy, and P. R. Roberts, "Practical application of the revised guidelines for the provision and assessment of nutrition support therapy in the adult critically Ill patient," *Nutrition in Clinical Practice*, vol. 31, 2016.

[25] P. Forsythe, "Probiotics and lung diseases," *Chest*, vol. 139, no. 4, pp. 901–908, 2011.

[26] E. Mortaz, I. M. Adcock, G. Folkerts, P. J. Barnes, A. Paul Vos, and J. Garssen, "Probiotics in the management of lung diseases," *Mediators of Inflammation*, vol. 2013, Article ID 751068, 1–10 pages, 2013.

[27] K. F. Rabe, S. Hurd, A. Anzueto et al., "Global strategy for the diagnosis, management, and prevention of chronic obstructive pulmonary disease," *American Journal of Respiratory and Critical Care Medicine*, vol. 176, no. 6, pp. 532–555, 2007.

[28] J. Nadigel, D. Préfontaine, C. J. Baglole et al., "Cigarette smoke increases TLR4 and TLR9 expression and induces cytokine production from CD8+T cells in chronic obstructive pulmonary disease," *Respiratory Research*, vol. 12, no. 1, p. 149, 2011.

[29] C. F. Vogelmeier, G. J. Criner, F. J. Martinez et al., "Global strategy for the diagnosis, management and prevention of chronic obstructive lung disease 2017 report," *Respirology*, vol. 22, no. 3, pp. 575–601, 2017.

[30] C. Zuany-Amorim, J. Hastewell, and C. Walker, "Toll-like receptors as potential therapeutic targets for multiple diseases," *Nature Reviews Drug Discovery*, vol. 1, no. 10, pp. 797–807, 2002.

[31] P. Wang, X. Han, B. Mo, G. Huang, and C. Wang, "LPS enhances TLR4 expression and IFN-γ production via the TLR4/IRAK/NF-κB signaling pathway in rat pulmonary arterial smooth muscle cells," *Molecular Medicine Reports*, vol. 16, no. 3, pp. 3111–3116, 2017.

[32] L. E. C. Alexander, S. Shin, and J. H. Hwang, "Inflammatory diseases of the lung induced by conventional cigarette smoke: a review," *Chest*, vol. 148, 2015.

[33] X. Y. Gu, X. Chu, X. L. Zeng, H. R. Bao, and X. J. Liu, "Effects of PM2.5 exposure on the Notch signaling pathway and immune imbalance in chronic obstructive pulmonary disease," *Environmental Pollution*, vol. 226, pp. 163–173, 2017.

[34] J. Fernandez, B. Silvan, R. Entrialgo-Cadierno et al., "Antiproliferative and palliative activity of flavonoids in colorectal cancer - ScienceDirect," *Biomedicine & Pharmacotherapy*, vol. 143, 2021.

[35] E. Küpeli Akkol, I. Tatlı Çankaya, G. Şeker Karatoprak, E. Carpar, E. Sobarzo-Sánchez, and R. Capasso, "Natural compounds as medical strategies in the prevention and treatment of psychiatric disorders seen in neurological diseases," *Frontiers in Pharmacology*, vol. 12, 2021.

[36] M. N. U. Chy, M. Adnan, M. R. Chowdhury et al., "Central and peripheral pain intervention by Ophiorrhizarugosa leaves: potential underlying mechanisms and insight into the role of pain modulators," *Journal of Ethnopharmacology*, vol. 276, 2021.

[37] M. A. Freitas, A. Vasconcelos, E. C. D. Goncalves et al., "Involvement of opioid system and TRPM8/TRPA1 channels

in the antinociceptive effect of Spirulina platensis," *Biomolecules*, vol. 11, no. 4, p. 592, 2021.

[38] A. J. Chakraborty, S. Mitra, T. E. Tallei et al., "Bromelain a potential bioactive compound: a comprehensive overview from a pharmacological perspective," *Life*, vol. 11, no. 4, p. 317, 2021.

[39] A. Reza, M. Adnan, M. A. Rahman, A. M. Tareq, and K. Alam, "Therapeutic potentials of syzygium fruticosum fruit (seed) reflect into an array of pharmacological assays and prospective receptors-mediated pathways," *Life*, vol. 11, no. 2, 2021.

[40] M. S. Bari, E. Haque, B. Romano et al., "Ethnomedicinal uses, phytochemistry, and biological activity of plants of the genus Gynura," *Journal of Ethnopharmacology*, vol. 271, 2021.

[41] O. Goni, M. F. Khan, M. M. Rahman et al., "Pharmacological insights on the antidepressant, anxiolytic and aphrodisiac potentials of Aglaonema hookerianum Schott," *Journal of Ethnopharmacology*, vol. 268, no. 12, 2021.

[42] Y. L. Ou and Z. Cai, "Clinical application research progress of peitu shengjin method in treating chronic obstructive pulmonary disease," *Clinical Journal of Traditional Chinese Medicine*, vol. 31, no. 008, pp. 1402–1405, 2019.

[43] N. P. Knyazheskaya, I. A. Baranova, and M. P. Fabrika, "Novel potentials for treatment and prevention of arvi in patients with chronic obstructive pulmonary disease," *Medical Council*, 2017.

[44] J. Gong, N. Chen, X. M. Hao, and H. Li, "Effect of peitu shengjin Recipe on nutritional states and immune functions of stable phase COPD patients," *Chinese Journal of Integrated Traditional and Western Medicine*, vol. 35, 2015.

[45] A. Khwaldeh, A. A. Siyam, A. A. Alzbeede, M. Farajallah, Z. Shraideh, and D. Badran, "Ameliorative effects of curcumin and caffeic acid against short term exposure of waterpipe tobacco smoking on lung, heart and kidney in mice," *Anatomy & Cell Biology*, vol. 54, no. 1, pp. 93–103, 2021.